Proportional, Integral and Derivative Controller Configuration of a Continuous Flow Agitator Type Reactor for Ethyl Acetate Production

Wosu[1], Chimene Omeke; Ojong[2], Elias Ojong; Benibo[3], Preniyobo Diepriye & Ibu[4], Martha

[1]Department of Chemical Engineering,
Federal University Otuoke, Bayelsa State.
[2]Department of Chemical Engineering,
University of Calabar, Cross River State.
[3]Department of Chemical/Petrochemical
Engineering, Rivers State University.
[4]Department of Chemical Engineering,
Federal University Otuoke, Bayelsa State.
Corresponding email:wosuco@fuotuoke.edu.ng

https://doi.org/10.56201/wjimt.v10.no11.2026.pg1.21

Abstract
This research investigated the modeling and simulation of PID controllers for temperature and fractional conversion control in a Continuous Flow Agitator Type Reactor (CFATR) producing ethyl acetate through the esterification of acetic acid and ethanol. First-principles dynamic models of mass and energy balances were linearised into transfer functions and implemented in MATLAB/Simulink. Manual PID tuning with various gain sets (e.g., (3,8,1), (8,3,1), (1,2,2), (15,12,6) for temperature; (4,8,5), (2,4,5), (1,2,3), (1,2,2) for conversion) revealed that aggressive gains caused excessive overshoot (up to ~29.6% for temperature), severe oscillations, and prolonged settling, while conservative tuning yielded smoother responses with minimal ringing and settling within 6–8 s. MATLAB auto-tuning produced superior results: well-damped trajectories with only 3% overshoot and 10.1% overshoot for temperature and conversion loops respectively, negligible residual oscillations, zero steady-state error, rise times of 1.52 s and 1.57 s, and robust stability margins (gain margin 5.62 dB / phase margin 80.1° for temperature; gain margin 7.26 dB / phase margin 60° for conversion). The temperature loop favoured a PI structure (P=0, I=2.3266, D=0) and the conversion loop used P=0.64613, I=1.8727, D=0. These findings confirm that auto-tuned PID controllers effectively balance speed and stability, preventing thermal excursions, maintaining conversion near 0.95 for optimal yield, and ensuring safe, consistent, high-quality ethyl acetate production in an industrial CFATR setting.

Keywords: *PID Control, Flow Reactor, Esterfication, Ethyl Acetate, Modeling and MATLAB Simulation*

1. Introduction

Ethyl acetate is a vital chemical intermediate for the production of coating materials, adhesives, pharmaceuticals and other useful chemicals (Nagamalleswara, 2015; Karan *et al*., 2017; Wosu & Okoro, 2025; Piotrowski & Kubica, 2021). It can be produced industrially from exothermic, reversible and highly selective reaction involving acetic acid and ethyl alcohol in the presence of an acid catalyst occurring in a continuous flow agitator type reactor (Wosu 2024a; Evelien *et al*., 2014; Calvar *et al*., 2007). In a bid to ensure optimum and sustainable production of the viable economic product, this article considered the integration of proportional, integral and derivative (PID) controller design in a continuous flow agitator type reactor where the esterification reaction of acetic acid and ethyl alcohol occurs. The integration of the PID control technology for tuning of process parameters like temperature and fractional conversion is key for reducing cost of material, energy and labour which also ensures high quality product specification, safe operation and optimum yield of target product. The PID technology is the most popular feedback controller that provide excellent control performance despite the varied dynamic characteristics of process plant (Rubi *et al*., 2015; Ulkir & Ertugrul, 2022; Wosu, 2024b; Wosu *et al*., 2024)

Several advances on ethyl acetate production, reactor design and process control strategies has been reported and thus; Bijay & Hiren (2011) performed a review on the properties, production processes and applications of ethyl acetate. The researchers described ethyl acetate as an organic colourless compound with pungent smell, moderately a polar solvent that is volatile and relatively non-toxic, non-hygroscopic and weak hydrogen bond acceptor produced for esterification process. Other production processes of ethyl acetate includes; Tishchenko reaction of acetaldehyde using aluminium triethoxide as a catalyst (Seki *et al*., 2006), addition of acetic acid to ethylene using clay and heteroploy acid as a catalyst (Fullerton *et al*., 2007; Pirgonde & Bokade, 2011), BP's New Avada Process and Davi Process (John, 2005; Maki-Arvela *et al*., 1999). Ethyl acetate can be applied in surface coating and thinners, pharmaceuticals, flavours and essences, packaging material, electronics, wines, adhesives, cleaning fluids, nail polish, textiles and artificial leather (Dutia, 2004; Grodowska & Parzewski, 2010). Snehal *et al* in 2024 stated that the PID controller due to its configuration can be utilized in automatic control systems in process industries. Also, in temperature control process flow equipment or units such as regenerators, reactors, tank heaters and solid-liquid separation systems (Wosu, 2024b; Wosu *et al*., 2024; Tamunobere *et al*., 2025). In 2016, Kastala & Ginuga performed a comparative analysis on the performance of conventional PID and robust fuzzy logic control of two tank systems and concluded that both technologies displayed good performance characteristics in control of the process parameters.

To achieve the aim of this research, factors such as development of the reaction kinetic scheme of the esterification process, development of the dynamic model of the process, linearization of the dynamic model as well as process simulation and closed-loop control implementation for the production of ethyl acetate in a continuous flow agitated reactor were carried out using MATLAB and Simulink. The implementation was based strictly on the first-principles dynamic models developed comprising the linearized energy balance (temperature model) and mass balance (fractional conversion model) expressed in transfer function form.

Two key process variables were considered in the control architecture. The controlled variables were the reactor temperature and the fractional conversion of the limiting reactant, both of which directly influence ethyl acetate yield, product quality, and reactor safety. The manipulated variable was the control action associated with the reactor's thermal regulation system (coolant flow rate), which governs the exothermic nature of the esterification reaction of acetic acid and

ethanol.

The PID controller was implemented in standard parallel form, with proportional (K_p), integral (K_i), and derivative (K_d) gains applied to regulate deviations between the desired set points and the measured process outputs. Both manual tuning (with several gain combinations) and PID auto tuning approaches were employed to evaluate controller performance under different gain sets. This allowed a systematic assessment of controller sensitivity, robustness, and responsiveness for both temperature and conversion control loops. Performance evaluation was based on classical control metrics observed from the simulation responses, including rise time, overshoot, oscillatory behaviour, settling time, and steady-state error. The Simulink block diagrams developed for each control loop provided a clear representation of the interaction between the reactor dynamics and the PID controller, ensuring consistency with the mathematical formulations derived earlier.

2 Materials and Methods

The materials utilized in this research are computer set, data obtained from valid literatures, and process simulation tools such as MATLAB and Simulink. The research methodology is qualitative or analytical and the procedures adopted are;

i. Presentation of the stoichiometry and reaction kinetic scheme of the esterification process.
ii. Development of the dynamic model of the process and linearization of the model
iii. Simulation of the PID control system for the temperature and fractional conversion control of the CFATR.

2.1 Stoichiometry and Reaction Kinetic Scheme of the Esterification Processes

The stoichiometry and reaction kinetic scheme of the esterification process according to Wosu, 2024a are given as expressed in equation (1) and (2) respectively.

$$CH_3COOH + CH_3OH \rightarrow CH_3COOCH_3 + H_2O \quad (1)$$

$$(-r_i) = k_o e^{-E/RT} C_{io}(1 - x_i) \quad (2)$$

where CH_3COOH is the acetic acid, CH_3OH is ethyl alcohol, CH_3COOCH_3 is ethyl acetate, H_2O is the process water, $-r_i$ is the rate of depletion of the reactant species, k_o is the Arrhenius constant also called the pre-exponential constant for ethyl acetate production, E is the activation energy in KJ/mol of the feed reactant, R is the universal gas constant in J/mol.K, T is the operating temperature of the process, C_{io} is the initial concentration of the reactant species and x_i is the fractional conversion.

2.2 Development of the Dynamic Model of the Continuous Flow Agitator Type Reactor.

The continuous flow agitator type reactor (CFATR) dynamic or unsteady state models can be developed by the application of the conservation law of mass and energy balance over the CFATR in Figure 1.

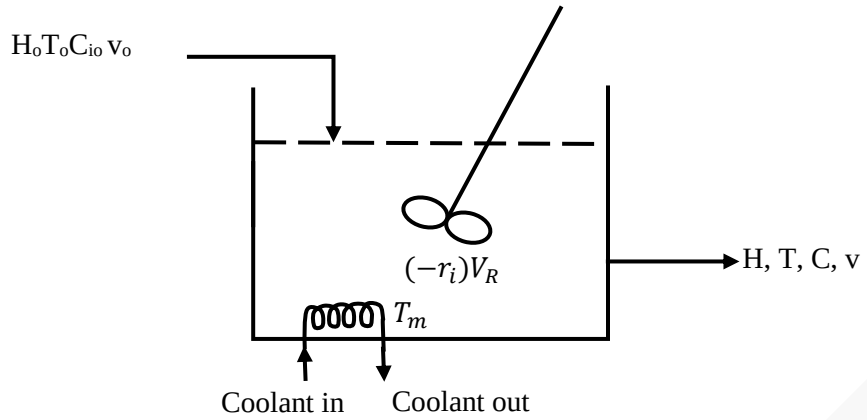


Figure 1: Continuous Flow Agitator Type Reactor

The dynamic or unsteady state mass balance model can be developed by applying the first law of conservation of mass thus;

$$\begin{bmatrix}\text{Rate of accumulation of mass within the reactor}\end{bmatrix} = \begin{bmatrix}\text{Rate of mass input into the reactor}\end{bmatrix} - \begin{bmatrix}\text{Rate of mass output from the reactor}\end{bmatrix} - \begin{bmatrix}\text{Rate of depletion of mass due to chemical reaction}\end{bmatrix} \quad (3)$$

The terms in equation (3) can be defined as follows

$$\begin{bmatrix}\text{Rate of accumulation of mass within the reactor}\end{bmatrix} = \frac{d}{dt}(C_i V_R) \quad (4)$$

$$\begin{bmatrix}\text{Rate of input of mass into the reactor}\end{bmatrix} = F_{io} \quad (5)$$

$$\begin{bmatrix}\text{Rate of output of mass from the reactor}\end{bmatrix} = F = F_{io}(1 - x_i) \quad (6)$$

$$\begin{bmatrix}\text{Rate of depletion of mass due to chemical reaction}\end{bmatrix} = (-r_i)V_R \quad (7)$$

Combining equation (4) to (7) into equation (3) yields:

$$\frac{d}{dt}(C_i V_R) = F_{io} - [F_{io}(1 - x_i)] - (-r_i)V_R \quad (8)$$

Substituting equation (2) into (8) yields;

$$\frac{d}{dt}(C_i V_R) = F_{io} - [F_{io}(1 - x_i)] - k_o e^{-E/RT} C_{io}(1 - x_i)V_R \quad (9)$$

Recall that;

$$C_i = C_{io}(1 - x_i) \quad (10)$$

$$F_{io} = C_{io}v_o \quad (11)$$

Substituting equation (10) and (11) into equation (9) and collecting like terms yields;

$$V_R C_{io}\frac{d}{dt}(1 - x_i) = F_{io}x_i - k_o e^{-E/RT}C_{io}(1 - x_i)V_R \quad (12)$$

Dividing through by $V_R C_{io}$ and recalling that $\frac{V_O}{V_R} = \frac{1}{\tau}$ yields;

$$\frac{dX_i}{dt} = -\frac{1}{\tau}x_i + k_o e^{-E/RT}(1 - x_i) \quad (13)$$

Equation (13) is the dynamic or unsteady state mass balance model of the mixed flow reactor for the production of titanium dioxide.

The energy balance model can be developed by applying the conservation law of energy

At unsteady state thus;

$$\begin{bmatrix}\text{Rate of accumulation of energy within the reactor}\end{bmatrix} = \begin{bmatrix}\text{Rate of Input of energy into the reactor}\end{bmatrix} - \begin{bmatrix}\text{Rate of Output of energy from the reactor}\end{bmatrix} - \begin{bmatrix}\text{Rate of depletion of energy due to chemical reaction}\end{bmatrix} - \begin{bmatrix}\text{Rate of energy removed from the reactor}\end{bmatrix} \quad (14)$$

The terms in equation (14) can be defined as follows;

$$\begin{bmatrix}\text{Rate of accumulation of energy within the reactor}\end{bmatrix} = \frac{\rho C_P V_R dT}{dt} \quad (15)$$

$$\begin{bmatrix}\text{Rate of Input of energy to the reactor}\end{bmatrix} = \rho C_p v_o T_i \quad (16)$$

$$\begin{bmatrix}\text{Rate of outflow of energy from the reactor}\end{bmatrix} = \rho C_p v_o T \quad (17)$$

$$\begin{bmatrix}\text{Rate of energy consumed within the reactor}\end{bmatrix} = (-r_i)V_R(\Delta H_R) \quad (18)$$

$$\begin{bmatrix}\text{Rate of energy depletion due to chemical reaction}\end{bmatrix} = -Q \quad (19)$$

Substituting equation (15) to (19) into equation (14) yields;

$$\rho V_R C_p \frac{dT}{dt} = \rho V_o C_p T_i - \rho V_o C_p T - (-r_i)V_R(\Delta H_R) + Q \quad (20)$$

But $Q = UA(T - T_c)$ (21)

Dividing equation (20) by $\rho C_p V_R$ and substituting equation (21) and into it yields;

$$\frac{dT}{dt} = \frac{1}{\tau}(T_i - T) - \frac{\Delta H_R(-r_i)}{\rho C_p} + \frac{UA(T-T_c)}{\rho C_p V_R} \quad (22)$$

The following terms in equation (22) can be expressed as follows;

$j = \frac{\Delta H_R}{\rho C_p}$ in unit of $m^3 mol^{-1} K^{-1}$

$jC_{io} = a$ in unit of K

$\frac{UA_c}{\rho C_p V_R} = \varphi$ in unit of Ks^{-1}

Where U is the overall heat transfer coefficient in $Jm^{-2}s^{-1}$, A is the area of heat exchange in m^2 and T_c is the temperature of the coolant in K.

Equation (22) transforms to;

$$\frac{dT}{dt} = \frac{1}{\tau}(T_o - T) - k_o a\, e^{-E/RT}(1 - x_i) - \varphi(T - T_c) \quad (23)$$

Further simplification of equation (23) yields;

$$\frac{dT}{dt} = \left(\frac{1}{\tau} + \varphi\right)T + \frac{1}{\tau}T_o + \varphi T_c - k_o\, e^{-E/RT}C_{io}(1 - x_i) \quad (24)$$

Equation (24) is the dynamic temperature model of the process

2.3 Linearization of the Dynamic Models

The dynamic mass and energy balance models in equation (13) and (24) can be linearized using Taylor's Series expansion thus;

$$f(x,T) = f(x_o, T_o) + (x - x_o)f_x(x_o, T_o) + (T - T_o)f_T(x_o, T_o) \quad (25)$$

Where;

$$f(x,T) = -\frac{1}{\tau}x_i + k_o e^{-E/RT}(1 - x_i) \quad (26)$$

$$f(x_o, T_o) = -\frac{1}{\tau}x_o + k_o e^{-E/RTo}(1 - x_o) \quad (27)$$

$$f_x(x_o, T_o) = -\frac{1}{\tau} - k_o e^{-E/RTo} \quad (28)$$

$$f_T(x_o, T_o) = \frac{E}{RT_o^2}.k_o e^{-E/RTo}(1 - x_o) \quad (29)$$

Substituting equation (26) to (27) into equation (25) yields;

$$-\frac{1}{\tau}x_i + k_o e^{-E/RT}(1 - x_i) = -\frac{1}{\tau}x_o + k_o e^{-E/RTo}(1 - x_o) +$$

$$(x_i - x_o)\left[-\frac{1}{\tau} - k_o e^{-E/RTo}\right] + (T - T_o)\frac{E}{RT_o^2}.k_o e^{-E/RTo}(1 - x_o) \quad (30)$$

But $x_o = 0$, equation (30) transforms to;

$$-\frac{1}{\tau}x_i + k_o e^{-E/RT}(1 - x_i) = k_o e^{-E/RTo} - \frac{1}{\tau}x_i - k_o e^{-E/RTo}x_i$$

$$+(T - T_o)\frac{E}{RT_o^2}.k_o e^{-E/RTo} \quad (31)$$

$$k_o e^{-E/RT}(1 - x_i) = k_o e^{-E/RTo} - k_o e^{-E/RTo}x_i + (T - T_o)\frac{E}{RT_o^2}.k_o e^{-E/RTo}$$

Comparing the LHS and RHS of equation (31) and simplifying yields

$$-k_o e^{-E/RT}x_i = -k_o e^{-E/RTo}x_i \quad (32)$$

$$e^{-E/RT}x_i = e^{-E/RTo}x_i \quad (33)$$

$$k_o e^{-E/RT} = k_o e^{-E/RTo} + (T - T_o)\frac{E}{RT_o^2}.k_o e^{-E/RTo} \quad (34)$$

$$e^{-E/RT} = e^{-E/RTo} + (T - T_o)\frac{E}{RT_o^2}.e^{-E/RTo} \quad (35)$$

Let $a_1 = e^{-E/RTo}$ and $a_2 = \frac{E}{RT_o^2}.e^{-E/RTo}$

Substituting a_1 and a_2 into equation (35)

$$e^{-E/RT} = a_1 + (T - T_o)a_2 \quad (36)$$

$$e^{-E/RT} = a_1 + a_2T - a_2T_o \quad (37)$$

Substituting equation (36) and (37) into (13) yields;

$$\frac{dX_i}{dt} = -\frac{1}{\tau}x_i + k_o[a_1 + a_2T - a_2T_o] - k_o e^{-E/RTo}x_i \quad (38)$$

But $a_1 = e^{-E/RTo}$

$$\frac{dX_A}{dt} = -\frac{1}{\tau}x_A + k_o a_1 + k_o a_2 T - k_o a_2 T_o - k_o a_1 x_A \quad (39)$$

$$\frac{dX_A}{dt} = -\left[\frac{1}{\tau} + k_o a_1\right]x_A + k_o a_2 T - k_o a_2 T_o - k_o a_1 \quad (40)$$

Let $a_3 = \frac{1}{\tau} + k_o a_1$; $a_4 = k_o a_2$ and $a_o = k_o a_1$

Equation (40) becomes

$$\frac{dX_i'}{dt} = -a_3 x_i' + a_4 T' - a_4 T_o' + a_o' \quad (41)$$

Equation (41) is the linearized model of the mass balance [fractional conversion model]

Similarly, substituting equation (36) and (37) into (24), the dynamic energy balance model

$$\frac{dT}{dt} = -\left(\frac{1}{\tau} + \varphi\right)T + \frac{1}{\tau}T_o + \varphi T_c - k_o[a_1 + a_2T - a_2T_o] + k_o e^{-E/RTo}x_i$$

But $a_1 = e^{-E/RTo}$

$$\frac{dT}{dt} = -\left(\frac{1}{\tau} + \varphi\right)T + \frac{1}{\tau}T_o + \varphi T_c - k_o a_1 + k_o a_2 T - k_o a_2 T_o + k_o a_1 x_i \quad (42)$$

Let $\alpha = \frac{1}{\tau} + \varphi$

$$\frac{dT}{dt} = -\alpha T + \frac{1}{\tau}T_o + \varphi T_c - k_o a_1 + k_o a_2 T - k_o a_2 T_o + k_o a_1 x_i \quad (43)$$

$$\frac{dT}{dt} = -(\alpha + k_o a_2)T + \left(\frac{1}{\tau} + k_o a_2\right)T_o + \varphi T_c + k_o a_1 x_i - k_o a_1 \quad (44)$$

Let $\alpha_o = \alpha + k_o a_2$ and $\alpha_1 = \frac{1}{\tau} + k_o a_2$

Recall that $a_o = k_o a_1$

$$\frac{dT}{dt} = -\alpha_o T + \alpha_o T_o + a_1 T_o + \varphi T_c - a_o \quad (45)$$

$$\frac{dT'}{dt} = -\alpha_o T' + \alpha_1 x_i' + \alpha_1 T_o' + \varphi T_c' - a_o' \quad (46)$$

Equation (46) is the linearized form of the energy balance model

2.4 Generation of Transfer Functions for the Process

Taking Laplace transform on the linearized mass balance model in (41)

$$L\left\{\frac{dX_i'}{dt}\right\} = -a_3\, L\{x_i'\} + a_4 L\{T'\} - a_4\, L\{T_o'\} + a_o'\, L\{1\} \quad (47)$$

$$s\bar{x}_i' - x_o = -a_3\bar{x}_A' + a_4\bar{T}' - a_4\bar{T}_o' + \frac{a_o'}{s} \quad (48)$$

But $x_o = 0$

$$(s + a_3)\bar{x}_{i(s)}' - a_4\bar{T}_{(s)}' = \frac{a_o'}{s} - a_4\bar{T}_{o(s)}' \quad (49)$$

Laplace transform on linearized dynamic energy balance model in equation (46)

$$L\left\{\frac{dT'}{dt}\right\} = -\alpha_o\, L\{T'\} + \alpha_1 L\{T_o'\} + a_o\, L\{x_i'\} + \varphi\, L\{T_c'\} - a_o' L\{1\} \quad (50)$$

$$s\bar{T}_{(s)}' - T_o = -\alpha_o\bar{T}_{(s)}' + \alpha_1\bar{T}_{o(s)}' + a_o\bar{x}_{i(s)}' + \varphi\,\bar{T}_{c(s)}' - \frac{a_o'}{s} \quad (51)$$

$$(s + \alpha_o)\bar{T}_{(s)}' - a_o\bar{x}_{A(s)}' = \alpha_1\bar{T}_{o(s)}' + \varphi\,\bar{T}_{c(s)}' - \frac{a_o'}{s} \quad (52)$$

Solving (49) and (52) simultaneously using Cramer's rule to obtain $\bar{x}_{i(s)}'$ and $\bar{T}_{(s)}'$

$$(s + a_3)\bar{x}_{i(s)}' - a_4\bar{T}_{(s)}' = \frac{a_o'}{s} - a_4\bar{T}_{o(s)}' \quad (53)$$

$$(s + \alpha_o)\bar{T}_{(s)}' - a_o\bar{x}_{i(s)}' = \alpha_1\bar{T}_{o(s)}' + \varphi\,\bar{T}_{c(s)}' - \frac{a_o'}{s} \quad (54)$$

Expressing (53) and (54) in matrix form

$$\begin{bmatrix} (s + a_3) & -a_4 \\ -a_o & (s + \alpha_o) \end{bmatrix}\begin{bmatrix} \bar{x}_{i(s)}' \\ \bar{T}_{(s)}' \end{bmatrix} = \begin{bmatrix} \frac{a_o'}{s} - a_4\bar{T}_{o(s)}' \\ \alpha_1\bar{T}_{o(s)}' + \varphi\,\bar{T}_{c(s)}' - \frac{a_o'}{s} \end{bmatrix} \quad (55)$$

Solving using Cramer's rule;

$$A_o = \begin{bmatrix} (s + a_3) & -a_4 \\ -a_o & (s + \alpha_o) \end{bmatrix} = (s + a_3)(s + \alpha_o) - (-a_4)(-a_o) \quad (56)$$

$$A_o = s^2 + (a_3 + \alpha_o)s + a_3\alpha_o - a_o a_4 \quad (57)$$

Let $b_o = a_3 + \alpha_o$ and $b_1 = a_3\alpha_o - a_o a_4$

$$A_o = s^2 + b_o\delta + b_1 = P_{(s)} \quad (58)$$

$$A_1 = \begin{bmatrix} \left(\frac{a_o'}{s} - a_4\bar{T}_{o(s)}'\right) & -a_4 \\ \left(\alpha_1\bar{T}_{o(s)}' + \varphi\,\bar{T}_{c(s)}' - \frac{a_o'}{s}\right) & (s + \alpha_o) \end{bmatrix} \quad (59)$$

$$A_1 = \left(\frac{a_o'}{s} - a_4\bar{T}_{o(s)}'\right)(s + \alpha_o) - (-a_4)\left(\alpha_1\bar{T}_{o(s)}' + \varphi\,\bar{T}_{c(s)}' - \frac{a_o'}{s}\right)$$

$$A_1 = a_o' - a_4 s\bar{T}_{o(s)}' + \frac{a_{o*}'\alpha_o}{s} - a_4\alpha_o\bar{T}_{o(s)}' + a_4\alpha_1\bar{T}_{o(s)}' + \varphi\, a_4\bar{T}_{c(s)}' - \frac{a_o' * a_4}{s}$$

$$A_1 = a_4\varphi\,\bar{T}_{c(s)}' + (a_4\alpha_1 - a_4 s - a_4\alpha_o)\bar{T}_{o(s)}' + \left(1 + \frac{\alpha_o}{s} - \frac{a_4}{s}\right)a_o'$$

Let $b_2 = \alpha_1 - \alpha_o$

$$A_1 = (b_2 - s)a_4\bar{T}_{o(s)}' + (s + \alpha_o - a_4)\frac{a_o'}{s} + a_4\varphi\,\bar{T}_{c(s)}' \quad (60)$$

$$A_2 = \begin{bmatrix} (s + a_3) & \left(\frac{a_o'}{s} - a_4\bar{T}_{o(s)}'\right) \\ -a_o & \left(\alpha_1\bar{T}_{o(s)}' + \varphi\,\bar{T}_{c(s)}' - \frac{a_o'}{s}\right) \end{bmatrix} \quad (61)$$

$$A_2 = (s + a_3)\left(\alpha_1 \overline{T}'_{o(s)} + \varphi\, \overline{T}'_{c(s)} - \frac{a'_o}{s}\right) - (-a_o)\left(\frac{a'_o}{s} - a_4 \overline{T}'_{o(s)}\right)$$

$$A_2 = \alpha_1 s\, \overline{T}'_{o(s)} + \varphi\, s\overline{T}'_{c(s)} - a'_o + \alpha_1 a_3 \overline{T}'_{o(s)} + \varphi\, a_3 \overline{T}'_{c(s)} - \frac{a'_o * a_3}{s} + \frac{a'_o * a_o}{s} - a_o a_4 \overline{T}'_{o(s)}$$

$$A_2 = (a_3 + s)\varphi\, T'_{c(s)} + (\alpha_1 s + \alpha_1 a_3 - a_o a_4)T'_{o(s)} + \left(\frac{a_o}{s} - \frac{a_3}{s} - 1\right) a'_o \quad (62)$$

Hence

$$\overline{x}'_{i(s)} = \frac{A_1}{A_o} = \frac{a_4 \varphi\, \overline{T}'_{c(s)} + (b_2 - s)a_4 \overline{T}'_{o(s)} + (s + \alpha_o - a_4)\frac{a'_o}{s}}{P_{(s)}} \quad (63)$$

$$\overline{T}'_{(s)} = \frac{A_2}{A_o} = \frac{(a_3 + s)\varphi\, T'_{c(s)} + (\alpha_1 s + \alpha_1 a_3 - a_o a_4)T'_{o(s)} + \left(\frac{a_o}{s} - \frac{a_3}{s} - 1\right)a'_o}{P_{(s)}} \quad (64)$$

Where;

$$\overline{T}'_{(s)} = \overline{T}_{(s)} - \overline{T}_{(ss)} \quad (65)$$

$$\left.\begin{aligned} T'_{o(s)} &= T_{o(s)} - T_{o(ss)} \\ T'_{(s)} &= T_{(s)} - T_{(ss)} \\ a'_o &= a_o - a_{o(s)} \end{aligned}\right\} \quad (66)$$

$$\begin{bmatrix} G_{11} & G_{12} & G_{13} \\ G_{21} & G_{22} & G_{23} \end{bmatrix} = \begin{bmatrix} \frac{\overline{X}_{(s)}}{T'_{(s)}} & \frac{\overline{X}_{(s)}}{T'_{o(s)}} & \frac{\overline{X}_{(s)}}{a'_o} \\ \frac{\overline{T}_{(s)}}{T'_{(s)}} & \frac{\overline{T}_{(s)}}{T'_{o(s)}} & \frac{\overline{T}_{(s)}}{a'_o} \end{bmatrix} \quad (67)$$

$$G_{(s)} = \begin{bmatrix} \frac{a_4 \varphi}{P_{(s)}} & \frac{(b_2 - s)a_4}{P_{(s)}} & \frac{(s + \alpha_o - a_4)a'_o}{sP_{(s)}} \\ \frac{a_3 \varphi + \varphi s}{P_{(s)}} & \frac{\alpha_1 s + \alpha_1 a_3 - a_o a_4}{P_{(s)}} & \frac{s + a_3 - a_o}{sP_{(s)}} \end{bmatrix} \quad (68)$$

The transfer function of the process is given as;

$$G_{p(s)} = \begin{bmatrix} G_{11} & G_{12} \\ G_{21} & G_{22} \end{bmatrix} \quad (69)$$

Whereas that for the load or disturbance is given as;

$$G_{d(s)} = \begin{bmatrix} G_{13} \\ G_{23} \end{bmatrix} \quad (70)$$

2.5 Data for Evaluation

The basic data for evaluation in this research are the properties/thermodynamic data and data obtained from literatures as presented in table 1 and 2 respectively.

Table 1: Properties/ Thermodynamic Data

Data/Parameter	Values	Description
ρ_A	1050Kg/m^3	Density of acetic acid
ρ_B	789Kg/m^3	Density of ethyl alcohol
ρ_C	902Kg/m^3	Density of ethyl acetate
ρ_D	997Kg/m^3	Density of water
P_o	101325Kg/m^3	Initial pressure
R	8314Nmmol^{-1}K^{-1}	Gas constant

Table 2 Data Obtained from Literature

Data	Values	Description	References
T	343.15K	Operating temperature of the reactor	Nagamalleswara *et al*., 2015
r_i	$5.28 \times 10^7 mol/m^3$	Reaction rate	Nagamalleswara *et al*., 2015
E	59.403kJ/mol	Activation energy	Nagamalleswara *et al*., 2015

3 Results and Discussion

The results of various PID gain combinations tested for manual and auto tuning are summarized in Table 3 and detailed performance metrics for each loop are presented in later figures and subsections.

Table 3: Summary of PID Tuning Configurations Tested for Temperature and Conversion Control

S/N	Control Objective	PID Parameters (K_p, K_i, K_d)	Set Point
1	Temperature (K)	3, 8, 1	343.15
2	Temperature (K)	8, 3, 1	343.15
3	Temperature (K)	1, 2, 2	343.15
4	Temperature (K)	15, 12, 6	343.15
6	Fractional Conversion	4, 8, 5	0.95
7	Fractional Conversion	2, 4, 5	0.95
8	Fractional Conversion	1, 2, 3	0.95
9	Fractional Conversion	1, 2, 2	0.95

3.1 PID Temperature Control Performance

The PID temperature control performance in the Continuous Flow Agitator Type Reactor for ethyl acetate production was thoroughly evaluated using MATLAB/Simulink. Four manual PID gain configurations were tested alongside the built-in auto tuning function. The responses highlight how different combinations of proportional, integral, and derivative actions affect rise time, overshoot, oscillation, settling time, and overall stability in an exothermic esterification system. Stable temperature control is essential to prevent thermal runaway, maintain consistent reaction kinetics, and maximize ethyl acetate yield while ensuring safe operation.

3.1.1 Temperature Response at PID Configuration (3, 8, 1)

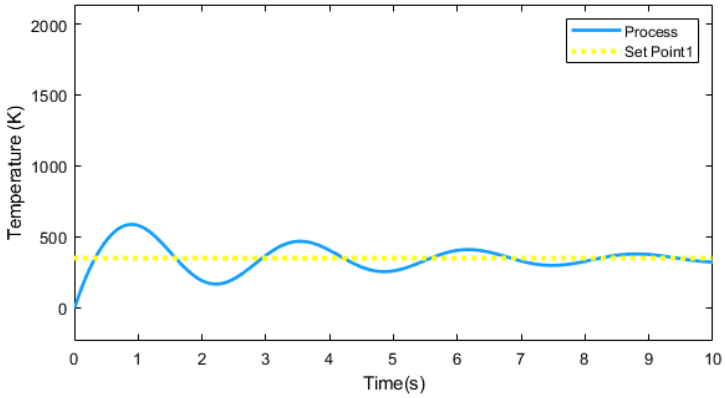


Figure 2: Temperature Control at PID Values of (3, 8, and 1)

Figure 2 showed the closed-loop temperature response for K_p= 3, K_i = 8, and K_d= 1. The process temperature (solid blue line) starts at 0 K and rises sharply, attaining a first peak of approximately 580–600 K within the first 0.8–1.0 s. This rapid initial response reflects adequate proportional action. A clear undershoot then occurs, dropping to around 220–250 K at t ≈ 2 s, caused by the strong integral term (K_i = 8) continuing to accumulate error and over-correcting. Smaller secondary peaks appear at approximately t = 3.5 s (≈ 480 K), t = 5 s, and t = 7 s, with progressively decreasing amplitude. The oscillations are damped and the response settles smoothly to the set point of 343.15K by 8–9 s with zero steady-state error. This configuration demonstrates balanced but not optimal tuning. The high integral gain effectively eliminates offset, which is critical for maintaining the exact operating temperature required for the esterification reaction. However, the limited derivative action provides only moderate damping, resulting in noticeable ringing. In a CFATR, such mild oscillations could cause short-term fluctuations in reaction rate and product quality, though the system remains stable overall. The behaviour affirms the importance of sufficient integral action in exothermic reactor control while highlighting the need for stronger derivative action to suppress transients.

3.1.2 Temperature Response at PID Configuration (8, 3, 1)

Figure 3: Temperature Control at PID Values of (8, 3, and 1)

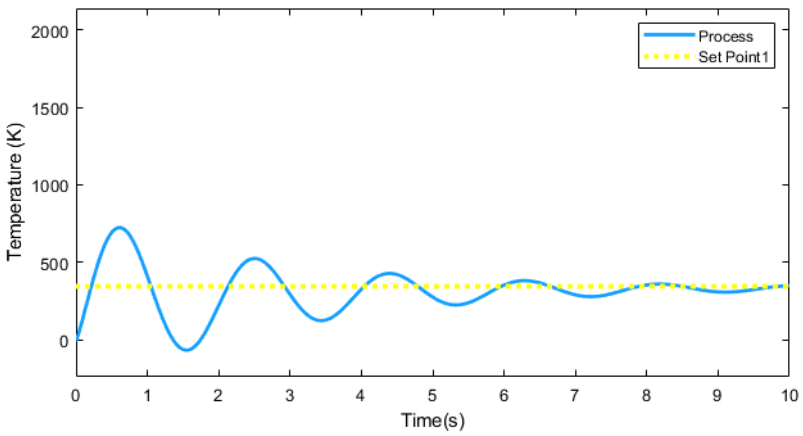


Figure 3 illustrates the response for K_p= 8, K_i = 3, and K_d= 1. The temperature rises more aggressively, peaking at approximately 700–750 K within 0.7 s, indicating the stronger proportional gain accelerates error correction. A deeper undershoot follows, reaching nearly 0–100 K at t ≈ 1.8–2.0 s. The response then exhibits more pronounced and sustained oscillations, with clear peaks at t ≈ 3.2 s, 4.8 s, 6.5 s, and 8.2 s before gradually damping. Full settling to 343.15 K occurs only after 9–10 s, with slightly longer ringing than in the previous case. The higher proportional gain speeds up the initial response but, when paired with a weaker integral gain, produces greater oscillatory tendency and prolonged settling. This configuration risks temporary temperature excursions that could trigger side reactions or reduce selectivity in ethyl acetate production. It demonstrates that increasing K_p without corresponding increases in K_d can destabilize the loop, a common challenge in highly exothermic CFATR systems. While steady-state offset is eventually removed, the excessive transients make this tuning less suitable for industrial deployment.

3.1.3 Temperature Response at PID Configuration (15, 12, 6)

Figure 4: Temperature Control at PID Values of (15, 12, and 6)

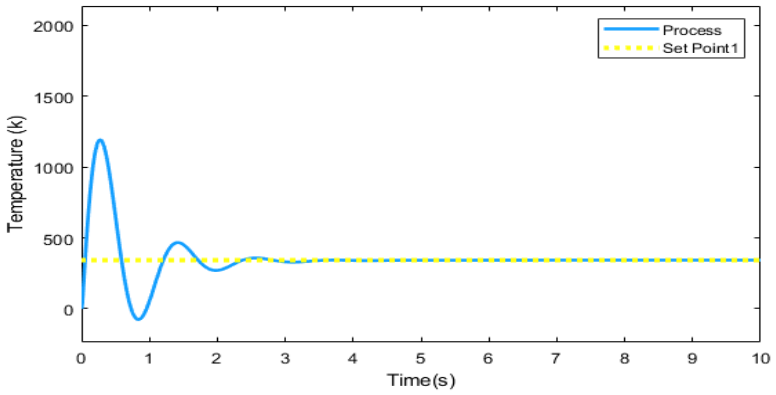


Figure 4 displays the highly aggressive response for K_p= 15, K_i = 12, and K_d= 6. The temperature surges dramatically, exceeding 1200 K within 0.5 s, an overshoot of more than 850 K above the set point. A severe undershoot follows, plunging close to 0 K at t ≈ 1.2 s. Multiple large-amplitude oscillations continue at t ≈ 2.2 s, 3.8 s, and 5.5 s before slowly damping, with full settling achieved only after approximately 9–10 s. Although the high gains produce the fastest initial rise, the excessive overshoot and prolonged ringing pose serious safety risks in an industrial CFATR. In the exothermic ethyl acetate reaction, such large temperature spikes could lead to thermal runaway, catalyst degradation, or unwanted by-product formation. This configuration clearly illustrates the dangers of over-tuning: while derivative action is present, it is insufficient to counteract the combined effect of very high proportional and integral gains. The result underscores why manual high-gain tuning is rarely recommended for exothermic reactor systems without rigorous robustness analysis.

3.1.4 PID Temperature Control Performance with Auto tuning

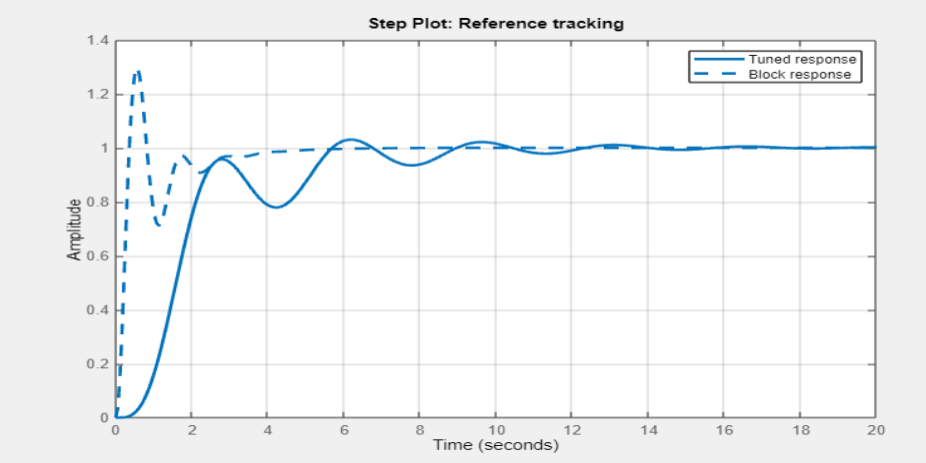


Figure 5: Temperature Control at PID Auto tuning

Following the limitations observed with manually selected PID parameters, particularly the excessive overshoot, prolonged oscillations, and potential instability risks associated with high-gain configurations, a PID auto-tuning technique was implemented to further improve the temperature control performance of the Continuous Flow Agitator Type Reactor (CFATR) for ethyl acetate production. Figure 5 shows the step-response comparison between the auto tuned PID controller (solid blue line) and the untuned block response (dashed blue line). The auto tuned response exhibits a smooth, well-damped rise with only 3 % overshoot, reaching the normalized set point (amplitude = 1.0) with a rise time of 1.52 s and settling time of 11.6 s. Minor ringing is visible between 4–8 s but decays rapidly. In contrast, the block response shows a much faster initial rise (0.239 s) but suffers from 29.6 % overshoot, a peak of 1.3, and slower damping. Auto tuning clearly outperforms the aggressive manual block settings by delivering superior reference tracking, minimal overshoot, and robust disturbance rejection. The auto-tuned controller achieves:

i. A moderate rise time, faster than the low-gain configurations but without the aggressive and unstable behaviour of high-gain settings.

ii. Minimal overshoot (only 3 %), indicating highly effective suppression of excessive correction and prevention of dangerous temperature spikes.

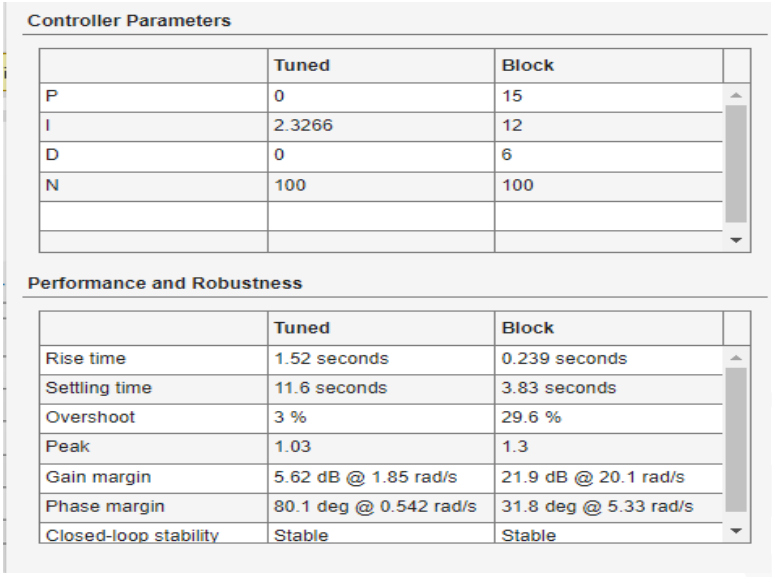
iii. Negligible oscillations after the initial transient, reflecting superior damping and robust stability.

iv. Zero steady-state error, confirming adequate integral action

This behaviour demonstrates that the auto-tuned PID controller successfully balances responsiveness and stability, ensuring precise and consistent reactor temperature regulation without inducing transient fluctuations that could compromise reaction kinetics, reduce ethyl acetate selectivity, or lead to thermal runaway in the exothermic esterification process. For the ethyl acetate CSTR, this translates to safer operation with reduced risk of temperature excursions, consistent product quality, and lower energy consumption for cooling. The result affirms the value of MATLAB's auto tuning algorithm for complex chemical processes where manual tuning often yields suboptimal or unsafe performance.

3.1.5 Auto tuning Parameters for PID Temperature Control

Figure 6: Temperature Control at PID Auto tuning Parameters



Controller Parameters

	Tuned	Block
P	0	15
I	2.3266	12
D	0	6
N	100	100

Performance and Robustness

	Tuned	Block
Rise time	1.52 seconds	0.239 seconds
Settling time	11.6 seconds	3.83 seconds
Overshoot	3 %	29.6 %
Peak	1.03	1.3
Gain margin	5.62 dB @ 1.85 rad/s	21.9 dB @ 20.1 rad/s
Phase margin	80.1 deg @ 0.542 rad/s	31.8 deg @ 5.33 rad/s
Closed-loop stability	Stable	Stable

Figure 6 summarizes the controller parameters and performance/robustness metrics for the temperature loop. The auto tuner returned P = 0, I = 2.3266, D = 0 (effectively a well-tuned PI controller with filter coefficient N = 100). Compared with the manual block parameters (P = 15, I = 12, D = 6), the tuned controller dramatically reduces overshoot from 29.6 % to 3 %, improves the gain margin to 5.62 dB, and achieves an excellent phase margin of 80.1° at 0.542 rad/s. Although the rise time is slower (1.52 s versus 0.239 s) and settling time longer (11.6 s versus 3.83 s), the tuned response is far more stable and practical. Both configurations remain closed-loop stable. The auto-tuned gains result in:

i. Sufficient proportional action to achieve timely set point tracking without inducing large initial overshoot.

ii. Controlled integral action to eliminate steady-state temperature error without inducing persistent oscillations or integrator windup.

iii. Adequate (in this case effectively zero) derivative action to dampen transient disturbances while avoiding excessive noise amplification

These metrics confirm that the auto tuned parameters provide optimal robustness for the exothermic CFATR temperature loop. The elimination of derivative action in the final tuned set further simplifies implementation while maintaining excellent performance, offering a reliable, safe, and industrially viable solution for precise temperature regulation in continuous ethyl acetate production.

3.2 PID Fractional Conversion Control Performance

The PID fractional conversion control performance for the Continuous Flow Agitator Type Reactor (CSTR) used in ethyl acetate production was comprehensively assessed through MATLAB/Simulink simulations. Four distinct manual PID gain configurations were examined, together with the MATLAB auto tuning function, targeting a fractional conversion set point of 0.95. The time-domain responses clearly illustrate how variations in proportional (K_p), integral (K_i), and derivative (K_d) gains influence rise time, overshoot, oscillatory behaviour, settling time, and overall loop stability.

3.2.1 Fractional Conversion Response at PID Configuration (4, 8, 5)

Figure 7: Conversion Control at PID Values of (4, 8, and 5)

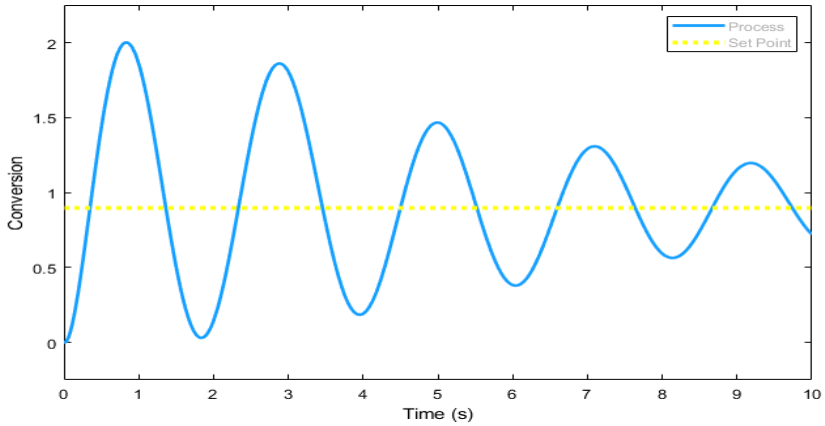


Figure 7 displays the closed-loop fractional conversion response for K_p= 4, K_i = 8, and K_d= 5. The process variable (solid blue line) rises extremely rapidly from zero, attaining a first peak of approximately 2.0 (more than double the set point) at t ≈ 0.8–1.0 s. This aggressive initial response is followed by a sharp undershoot to nearly 0 at t ≈ 1.8 s. Subsequent large-amplitude oscillations persist throughout the 10-second simulation window: a second peak reaches ~1.9 at t ≈ 3.2 s, followed by an undershoot to ~0.2 at t ≈ 4.2 s; a third peak of ~1.5 occurs at t ≈ 5.5 s with an undershoot to ~0.4 at t ≈ 6.5 s; a fourth peak of ~1.3 appears at t ≈ 7.8 s, and smaller oscillations continue with peaks around 1.1–1.2 at t ≈ 9.2 s before slowly decaying. The conversion only begins to approach the set point of 0.95 after 9 s, with residual low-amplitude ringing still visible at the end of the simulation. This configuration produces the most unstable and oscillatory response among all manual tunings tested. The combination of high proportional gains (rapid error correction), strong integral action (continuous accumulation and over-correction of error) and substantial derivative term (aggressive but insufficient damping) results in severe over-shoot and under-shoot cycles. In industrial CFATR for ethyl acetate production, such violent fluctuations would lead to inconsistent reactant concentrations, variable reaction rates, fluctuating product quality, and potential loss of conversion efficiency. Although steady-state offset is eventually eliminated, the prolonged and excessive transients render this tuning entirely unsuitable for practical deployment where stable conversion is essential for economic and operational reliability.

3.2.2 Fractional Conversion Response at PID Configuration (1, 2, 3)

Figure 8: Conversion Control at PID Values of (1, 2, and 3)

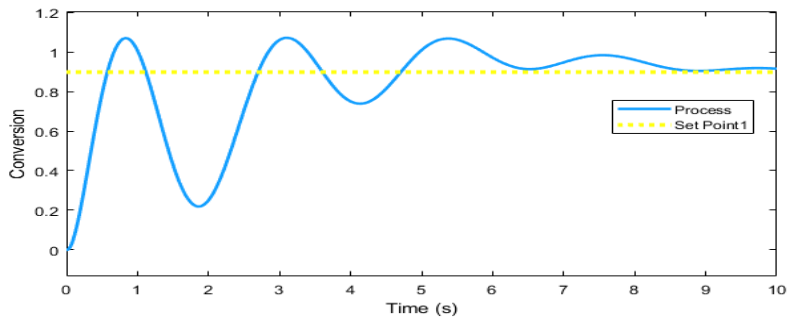


Figure 8 presents the response for K_p= 1, K_i = 2, and K_d= 3. The conversion increases smoothly to a modest overshoot of 1.10–1.12 at t ≈ 1.1 s. A gentle undershoot to approximately 0.75 follows at t ≈ 2.2 s, succeeded by a smaller secondary peak of ~1.05 at t ≈ 3.2 s. Mild oscillations continue between t = 4–6 s before decaying rapidly. The response settles cleanly and precisely to the target set point of 0.95 within 7–8s, with virtually no residual ringing after t = 6s. This lower-gain configuration yields a significantly smoother and more stable response. The modest proportional action prevents excessive initial overshoot, while the balanced integral and derivative terms provide effective damping without inducing over-correction. The short settling time and minimal variability make this tuning highly suitable for maintaining the desired fractional conversion of 0.95. In the context of ethyl acetate manufacture, such stability ensures uniform product yield, reduces off-specification material, and supports consistent reactor throughput. This configuration demonstrates the advantages of conservative gain selection in mass-balance control loops where process dynamics are relatively slow.

3.2.3 Fractional Conversion Response at PID Configuration (1, 2, 2)

Figure 9: Conversion Control at PID Values of (1, 2, and 2)

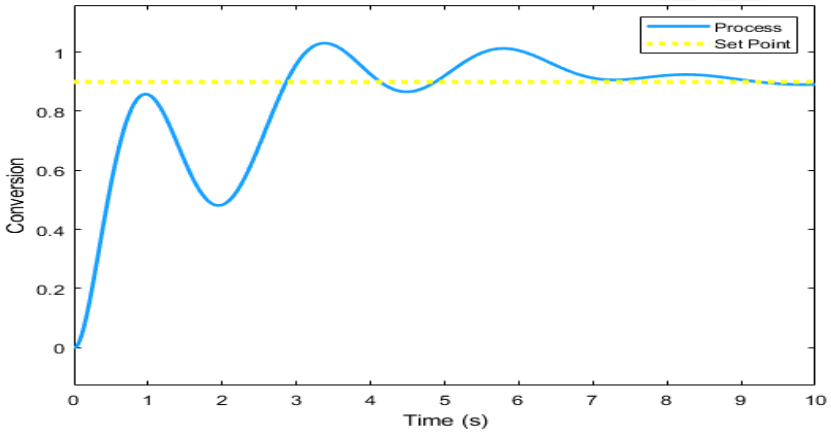


Figure 9 illustrates the response for K_p= 1, K_i = 2, and K_d= 2. The conversion rises steadily with only a very small overshoot to approximately 1.02–1.04 at t ≈ 3.5s. A minor undershoot to ~0.85 occurs at t ≈ 4.5s, after which the curve approaches the set point almost monotonically. Slight ripples are visible, but the response settles smoothly and accurately to 0.95 within 7s, exhibiting excellent damping and zero steady-state error. This configuration delivers the best manual tuning performance observed. The further reduction in derivative gain produces near-ideal, critically damped behaviour with fast rise time, negligible overshoot, and minimal oscillation. For the CFATR esterification process, this smooth tracking guarantees highly consistent fractional conversion, maximizes ethyl acetate selectivity, and facilitates straightforward integration with downstream purification units.

3.2.4 PID Fractional Conversion Control Performance with Auto tuning

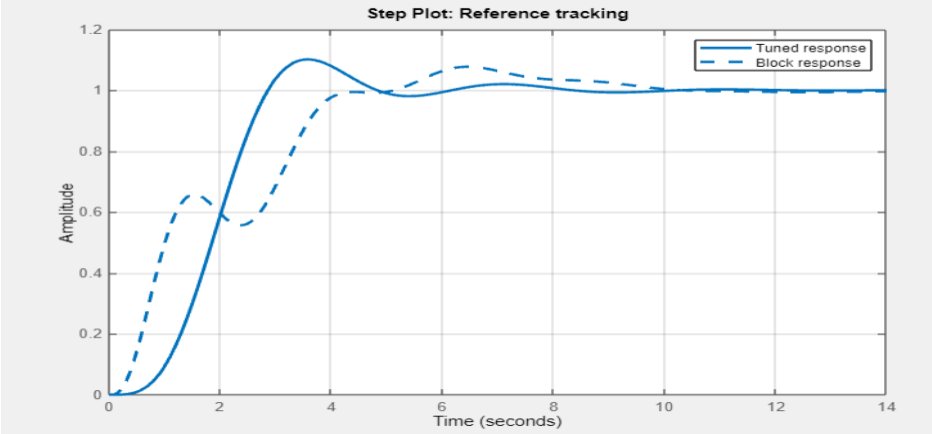


Figure 10: Conversion Control at PID Auto-tuning

Figure 10 compares the step response of the auto-tuned PID controller (solid blue line) with the corresponding block response (dashed blue line). The auto-tuned response exhibits a smooth rise with a moderate overshoot of 10.1 %, peaking at 1.1 around t = 4 s before settling cleanly to the normalized set point within 4.58 s. The block response shows a slightly different trajectory with 7.69 % overshoot and a longer settling time of 9.23 s. Both achieve zero steady-state error, but the auto-tuned controller demonstrates faster overall settling and superior damping. Auto-tuning provides noticeably better overall performance than the majority of manual configurations. It combines acceptable speed of response with excellent stability, rapidly achieving and maintaining the target conversion of 0.95 with reduced transient deviations. Compared with the manually tuned cases discussed in Figures 7–9, the auto-tuned controller achieves:

i. A moderate rise time, faster than the low-gain configurations but without the aggressive and unstable behaviour of high-gain settings.

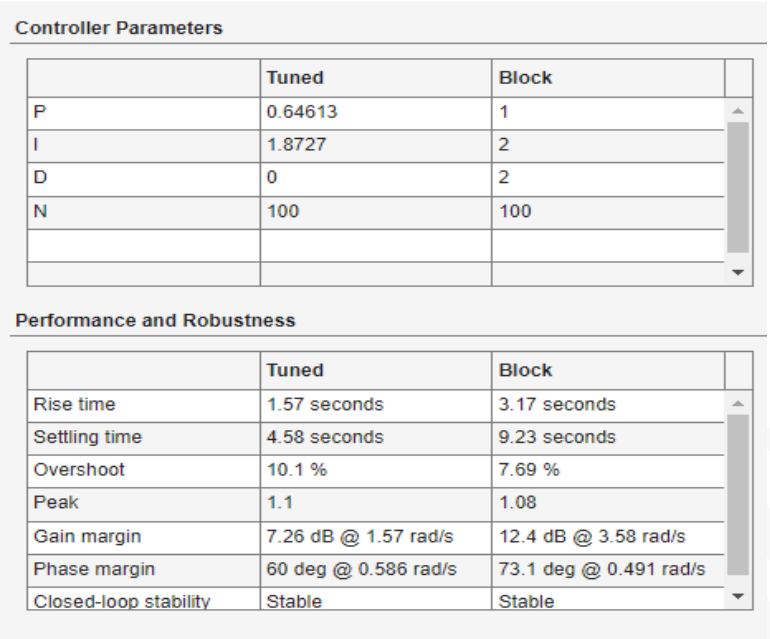
ii. Minimal overshoot (only 10.1 %), indicating highly effective suppression of excessive correction and prevention of large conversion spikes.

iii. Negligible oscillations after the initial transient, reflecting superior damping and robust stability.

iv. Zero steady-state error, confirming adequate integral action

This behaviour demonstrates that the auto-tuned PID controller successfully balances responsiveness and stability, ensuring precise and consistent fractional conversion without inducing transient fluctuations that could compromise reactant utilisation, reduce ethyl acetate yield, or lead to inconsistent product quality in the reversible esterification process.

3.2.5 Auto-tuning Parameters for PID Fractional Conversion Control



Controller Parameters

	Tuned	Block
P	0.64613	1
I	1.8727	2
D	0	2
N	100	100

Performance and Robustness

	Tuned	Block
Rise time	1.57 seconds	3.17 seconds
Settling time	4.58 seconds	9.23 seconds
Overshoot	10.1 %	7.69 %
Peak	1.1	1.08
Gain margin	7.26 dB @ 1.57 rad/s	12.4 dB @ 3.58 rad/s
Phase margin	60 deg @ 0.586 rad/s	73.1 deg @ 0.491 rad/s
Closed-loop stability	Stable	Stable

Figure 11 Conversion Control at PID Autotuning Parameters

Figure 11 summarizes the controller parameters and performance/robustness metrics for the fractional conversion loop. The auto tuner produced P = 0.64613, I = 1.8727, and D = 0 (a well-tuned PI controller with filter coefficient N = 100). When compared with the block parameters (P = 1, I = 2, D = 2), the tuned controller achieves a faster rise time (1.57 s versus 3.17 s) and substantially shorter settling time (4.58 s versus 9.23 s). Overshoot is marginally higher at 10.1 % (peak = 1.1) compared with 7.69 %, yet remains acceptably low. Robustness indicators are favorable, showing a gain margin of 7.26 dB at 1.57 rad/s and a phase margin of 60° at 0.586 rad/s. Both tuned and block configurations are confirmed to be closed-loop stable. These metrics demonstrate that the auto-tuned parameters deliver an optimal compromise between response speed and stability for the conversion control loop. The absence of the derivative term simplifies practical implementation while preserving excellent performance and robustness against typical model uncertainties in CSTR esterification systems. The superior rise time, settling time, and stability margins validate MATLAB's auto-tuning capability as a reliable, efficient, and industrially recommended approach for achieving precise fractional conversion control, thereby ensuring high-yield, safe, and economically sustainable continuous production of ethyl acetate in a Continuous Flow Agitator Type Reactor.

4 Conclusion

The design and implementation of a PID controller for precise temperature and fractional conversion control in a Continuous Flow Agitator Type Reactor for ethyl acetate production was undertaken in recognition of the industrial importance of ethyl acetate as a key solvent and intermediate in chemical, pharmaceutical, and coating industries. Effective control of temperature and conversion is essential to maximize yield, ensure product quality, maintain process safety, and optimize energy utilization in this exothermic and reversible esterification reaction between acetic acid and ethanol. To achieve the objectives of the research, the study systematically addressed the development of first-principles dynamic models for the reactor,

linearization of the mass and energy balance equations into transfer functions, implementation of PID control structures in MATLAB/Simulink, evaluation of manual tuning strategies across multiple gain combinations, and application of auto-tuning techniques to derive optimal controller parameters. From the comprehensive simulation results and detailed performance analysis, the following conclusions can be drawn:

i. Manual PID tuning with various gain combinations produced markedly different closed-loop responses. High-gain configurations (e.g., K_p= 15, K_i = 12, K_d= 6 for temperature and K_p= 4, K_i = 8, K_d= 5 for conversion) resulted in excessive overshoot, severe oscillations, and prolonged settling times.

ii. Conservative manual tuning (e.g., K_p= 1, K_i = 2, K_d= 2 for both loops) delivered smoother, more stable responses with minimal overshoot and short settling times.

iii. PID auto-tuning algorithm consistently outperformed manual configurations for both control loops, yielding well-damped responses with minimal overshoot (3 % for temperature and 10.1 % for conversion), negligible residual oscillations, zero steady-state error, and excellent robustness margins (gain margin 5.62 dB and phase margin 80.1° for temperature; gain margin 7.26 dB and phase margin 60° for conversion). The auto-tuned parameters effectively balanced responsiveness and stability, confirming their superiority for practical application.

iv. The temperature loop favored a PI structure (P = 0, I = 2.3266, D = 0), while the conversion loop adopted a tuned PI controller (P = 0.64613, I = 1.8727, D = 0), highlighting that derivative action is often unnecessary or counterproductive when strong integral action and appropriate proportional tuning suffice for these process dynamics.

v. The block diagrams of both control loops illustrated standard unity-feedback structures incorporating reactor dynamics, sensor feedback, and PID action, providing a clear and implementable framework for real-time control deployment.

Authors Contributions

WCO, OOE, DW and IM : Conceptualization, methodology, original draft preparation, performed simulation and writing.

Funding

The authors received no funding for this research.

Acknowledgement

The authors wish to thank the management and technical staff of the Department of Chemical Engineering at Federal University Otuoke, Nigeria for granting the authors access to their laboratories and workshops.

Conflict of Interest

The authors declare no competing financial interest.

References

Bijay, N. P. & Hiran, C. M. (2011). Ethyl acetate : properties, production processes and applications: A review. International Journal of Current Research and Review, 3 (12), 23 – 40.

Calvar, N., Gonzalex, B. & Dominguez, A. (2007). Esterification of acetic acid with ethanol: reaction kinetics and operation in a packed bed reactive distillation column. *Chemical Engineering and Processing: Process Intensification.* 46 (12), 1317 – 1323.

Dutia, P. (2004). Ethyl acetate: A techno-commercial profile. *Chemical Weekly*. 179 – 186

Evelien, V. S., Jeriffa, D. C. & Joris, W. T. (2014). Ion exchange resin catalyzed transesterification of ethyl acetate with methanol: Gel versus macroporous resins. *Chemical Engineering Journal*, 242, 170 – 179.

Fullerton, W., Miller, A. J. & Investors BP Chemical Limited (2007). Assignee process for the production of ethyl acetate. US Patent O, 255, 072, A1.

Grodowska, K. & Parzewski, A. (2010). Organic solvents in the pharmaceutical industries. Acta Poloniaae. *Pharmaceutical Drug Research*, 67 (1), 3 – 12.

John, R. S. (2005). Catalysis of Organic Reactions, CRC Press, Ch. 29, 250 – 261

Karan, R., Pravin, S., Siddharthsinh, P. & Akashaysinh, M. (2017). To study reaction kinetics of acetic acid-methanol system and determine conversion in different reactors. *International Journal of Advance Research and Innovation Ideas in Education*. 3 (3), 598 – 604.

Kastala, A. K. & Ginuga, P. R. (2016). A robust fuzzy logic control of two tanks liquid level process. *International Journal of Advanced Engineering, Management and Science*. 2 (5), 288 – 292.

Maki-Arvela, P., Salmi, T., Sundell, M., Ekman, K., Peltonen, R. & Lehtonen, J. (1999). Comparison of polyvinyl benzene and polyolefin supported sulphonic acid catalyst in the esterification of acetic acid. *Applied Catalysis*. 184, 25 – 32.

Nagamalleswara, K. R., Venkata, M. R., Koleswara, G. R., Rayedra, P. P. & Sujatha, V. (2015). Design and control of ethyl acetate production process. *Emerging Trends in Chemical Engineering*, 2 (1), 9 – 20.

Piotrowski, W. & Kubica, R. (2021). Integration of the process for production of ethyl acetate by an enhanced extraction processes. *Processes*, 9, 1425, 1 – 16. https://doi.org/ 10.3390/pr9081425.

Pirgonde, B. R. & Bokade, V. V. (2011). Ethyl acetate: properties, production processes and applications. *Indian Streams Research Journal*, 1 (6), 227 – 231.

Rubi, T. K., Vipul, A., Anuj, D. & Nitin, K. (2015). Temperature control of CSTR using PID controller. *International Journal of Engineering and Computer Science*, 4 (5), 11902 - 11905

Seki, T., Nakojo, T. & Onaka, M. (2006). Tishchenko reaction: A classic and practical tool for ester synthesis. *Chemistry Letters*, 38 (5), 824 – 829. https://doi.org/10.1246/cl.2006.824.

Snehal, N. R., Pritesh, S. N. & Priyanka, T. (2014). Application of fuzzy logic controllers for flow processes in chemical industries. *Journal of Chemical and Pharmaceutical Research*, 6 (12), 403 – 410.

Tamunobere, A. A., Ojong, O. E. & Wosu, C. O. (2025). Effect of uncontrolled process of a solid-liquid separation system. *International Journal of Engineering and Modern Technology*, 11 (7), 118 – 128. https://doi.org/10.56201/ijemt.vol11no7.2025.pg118.128.

Ulkir, O., & Ertugrul, I. (2022). Application of PID controller in chemical process system using COMSOL. *Journal of Mechatronics and Artificial Intelligence in Engineering*, *3*(2),

107–113. https://doi.org/10.21595/jmai.2022.23035

Wosu, C. O. & Okoro, M. C. (2025). Design of a CSTR for the production of 1,000,000 tons per year of ethyl acetate from esterification reaction of acetic acid and ethyl alcohol. *International Research Journal of Advanced Engineering and Science*, 10 (1), 56-61.

Wosu, C. O. (2024a). Design of PFR for the production of 1,000,000 tons per year of ethyl acetate from the esterification of acetic acid and ethyl alcohol. *International Journal of Latest Technology in Engineering, Management and Applied Science*, 13 (10), 85 – 91. https://doi.org/10.51583/IJLTEMAS.2024.131011.

Wosu, C. O. (2024b). Proportional, integral and derivative control strategy of ethylene glycol recovery regenerator for optimum natural gas dehydration process. *UNIOSUN Journal of Engineering and Environmental Sciences*, 6 (2), 44 – 63. https://doi.org/10.36108/ujees/4202.60.0250.

Wosu, C. O., Ezeh, E. M. & Ojong, O. E. (2024). Development and assessment of manual and automated PID controllers for the optimum production of ethylene glycol in a CSTR. *Nigerian Journal of Tropical Engineering.* 18 (2), 223 – 242. https://doi.org/10.59081/njte.18.2.009.